Age-dependent multi-hazard fragility functions
of operating offshore wind turbines

Ziliang Zhang – University of Bristol, Bristol, UK, e-mail: zz17635@bristol.ac.uk

Raffaele De Risi – University of Bristol, Bristol, UK, e-mail: raffaele.derisi@bristol.ac.uk

Anastasios Sextos – University of Bristol, Bristol, UK, e-mail: a.sextos@bristol.ac.uk

Abstract: This study develops age-dependent, wind–seismic fragility functions of an operational monopile-supported NREL 5 MW offshore wind turbine (OWT) considering stochastic loads of wind, wave and earthquake, as well as stochastic site and structural properties. From a geotechnical earthquake engineering perspective, OWT ageing is deemed to be caused by support-structure corrosion and foundation scour. A set of established OWT multi-hazard fragility assessment procedures was then performed to obtain fragility surfaces for a life cycle of 40 years. Results indicated that the multi-hazard fragility of an OWT is age-dependent, while degradation of the turbine-soil system integrity generally develops fast and then slows over time. It was also found that the OWT's probability of failure under the simultaneous design-level wind, wave and seismic inputs doubles after a typical 25-year design life.

Keywords: NREL 5 MW reference OWT; ageing; scour; corrosion; soil-structure interaction.

1. Introduction

Offshore wind turbine (OWT) supported by monopile foundation is a popular typology that is used in more than 80% of today's constructed units in shallow waters (< 30 m) due to its simple and robust design (WindEurope 2020). Its performance subjected to the adverse combination of multiple loads, including wind, wave and earthquakes, has been extensively studied both experimentally and numerically. Non-negligible, if not critical, structural demands were found possible due to the inclusion of multi-hazard modelling (Zheng et al. 2015; Katsanos et al. 2017) and the consideration of soil-structure interaction (Gelagoti et al. 2019). Some studies reflected these multi-hazard risks probabilistically in terms of multivariable fragility functions (Asareh et al. 2016; Martín del poCam and Pozos-Estrada 2020). The authors have also provided recommendations on the appropriate selection of statistical regression models and intensity measure combinations for this purpose (Zhang et al. 2022). Yet, an aspect that has not been addressed in detail is that structures deteriorate over time as their fragility may deviate substantially from the original state (Ghosh and Padgett 2010). To date, age-dependent multi-hazard fragility surfaces have rarely been assessed for operating monopile-supported OWTs, which is a major importance given that many wind farm owners are currently looking for mechanical refurbishment and lifetime extension of their ageing units. In this study, we present how the multi-hazard fragility surface of a typical operating OWT may evolve with age and how this may affect the time-dependent probability of failure. This was done by repeating a cloud-based multi-hazard fragility assessment process for multiple times, during which the model parameters governing the long-term OWT tower corrosion and foundation scour were stochastically sampled as functions of age. The results quantify the evolution of structural integrity in time.

2. Numerical modelling and analyses

2.1. Characterisation of the site and the structure

The NREL 5MW reference OWT (Jonkman et al. 2009) with its standard turbine/tower geometry and material properties was used in this study (Fig. 1a). The transition piece and the monopile was modelled as a steel cylinder of 6.0 m diameter and 0.060 m uniform wall-thickness. The seabed was situated 20.0 m deep below the mean sea level (MSL) and the monopile was embedded 36.0 m into the soil. The soil profile was assumed homogenous and was characterised by nominal values of unit weight γ_{soil} = 18.0 kN/m^3, Poisson's ratio ν_{soil} = 0.25, internal friction angle φ_{soil} = 35.0 °, and pile-tip shear modulus $G_{soil,t}$ = 60000 kPa. Rayleigh damping ζ = 3 % was adopted for the first two lateral vibration modes of the OWT (De Risi et al. 2018).
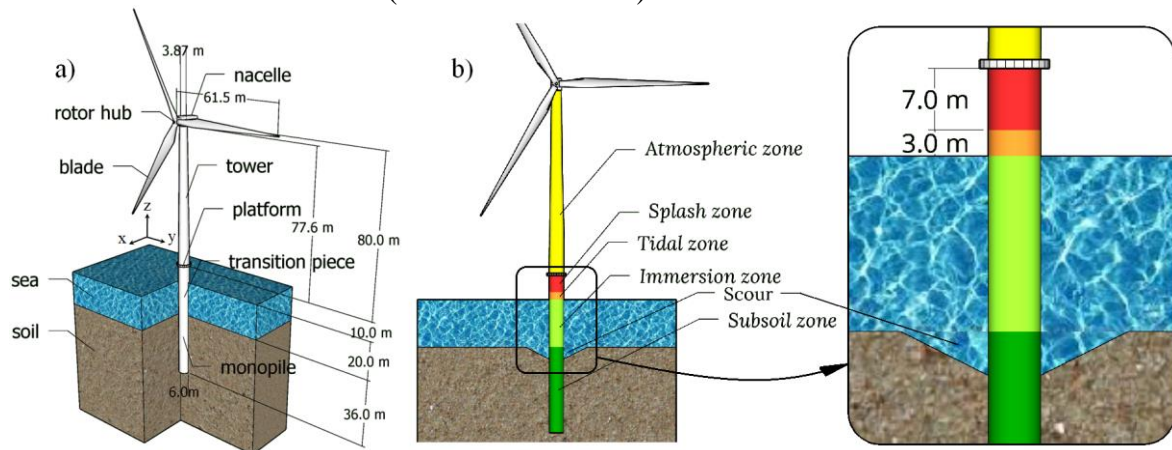

Fig. 1 –OWT geometry (a) and zones of corrosion and foundation scour (b).

Beam-on-nonlinear-Winkler-spring idealizations of the OWT were implemented in earthquake engineering specialization software OpenSees v3.2.0 (McKenna 2011), whilst the aero-hydro-servo-elastic simulator OpenFAST v2.3.0 (NREL 2020) was used in to individually calibrate each wind and wave input time histories in a corresponding pair of base-fixed OWT models. This process ensured the accuracy of wind and wave inputs before they were used in the subsequent OpenSees nonlinear time history analysis framework. A suite of appropriately selected (Katsanos et al. 2014) 300 earthquake records exhibiting a breadth of different ground motion characteristics was implemented to ensure unbiased estimate of structural performance.

Four established engineering demand parameters (EDPs) were sourced from the literature to describe failure criteria associated to two limit states. Two kinematics EDPs were used to define the serviceability limit state (SLS), namely, the tower-top chord rotation r_{top} and the tower-top lateral acceleration a_{top}. A threshold of ±0.5 ° was prescribed for r_{top} (De Risi et al. 2018) and a threshold of 0.6 m/s^2 was prescribed for a_{top} (Ramachandran et al. 2017). Ultimate limit state (ULS) was defined by the other two stress-related EDPs, namely the Von Mises equivalent design stress $\underline{\sigma}_{eq}$ and the Eurocode-compliant buckling-check stresses (CEN (European Committee for Standardisation) 2007), which were monitored along the perimeter and elevation of the entire OWT support-structure. The nominal yield strength of steel was taken as f_y = 3.55×10^5 kPa in order to calculate the above two stress related EDPs. For each limit state, failure was identified when the demand to capacity ratio Y exceeds unity.

2.2. Characterisation of OWT ageing

Deterioration of an OWT may occur in terms of fatigue of connections (Do et al. 2015), ageing of mechanical components (Rezamand et al. 2020), ageing of blades (Papi et al. 2021), and degradation of the soil-foundation system. Some of these phenomena can compromise wind energy production while others threaten structural safety. From an geotechnical earthquake engineering perspective, the deterioration of the soil-foundation-structure system is being focused herein, which mainly includes stiffening (Lai et al. 2020) or softening (Bisoi and Haldar 2014) of the soil-foundation system, as well as marine corrosion of the support-structure (Price and Figueira 2017).

2.2.1. Support-structure corrosion

Uniform general corrosion (Price and Figueira 2017) of the OWT support-structure was adopted in this study, for which the corrosion loss can be represented in finite-element models in terms of a uniformly reduced wall-thickness of the support-structure. A total of five corrosion zones (Yang et al. 2019) was defined along the elevation of the OWT support-structure, namely atmospheric zone, splash zone, tidal zone, immersion zone and subsoil zone [Fig. 1(b)]. Different corrosion models were assigned to each corrosion zone [Fig. 2(a)]. The linear corrosion model (Melchers 1999) was used for atmospheric, immersion, and subsoil zones, whereas a Weibull distribution formulated corrosion model proposed by (Qin and Cui 2003) was used for splash and tidal zones. In this study, corrosion models were assumed to be governed by two parameters, coating life $t_{coating}$ and maximum corrosion depth at 40 years d_{corr} [Fig. 2(a)].
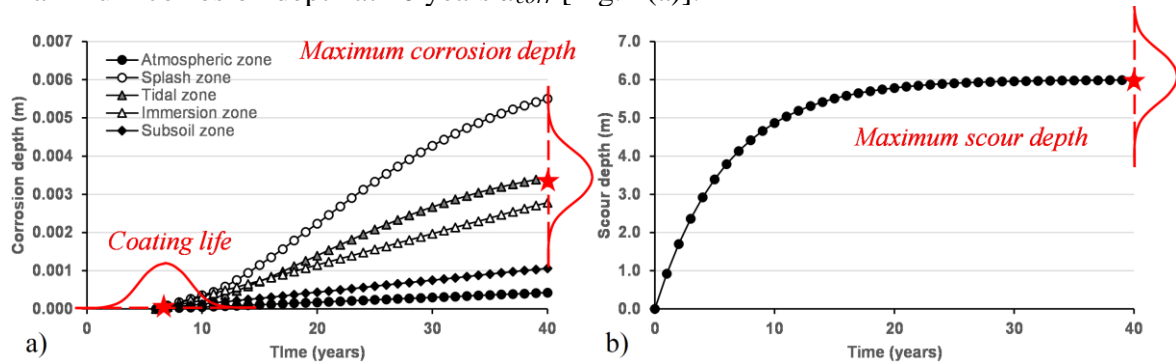

Fig. 2 – Illustration of the temporal evolution of: a) corrosion depth, b) scour depth. Corrosion and scour modal parameters assigned with randomness are indicated on the figures.

2.2.2. Foundation scour

Foundation scour results in the removal of sediment from around the subsea monopile foundation, hence, can affect the dynamic characteristics of the overall soil-foundation-structure system. The shape of the curve defining the temporal evolution of local scour depth [Fig. 2(b)] was defined by (DNV 2007). It was assumed that scour was governed by a single parameter, maximum scour depth at 40 years d_{scour}. The presence of foundation scour was modelled explicitly in the OpenSees seismic analysis models in terms of embedment reduction as elaborated in (Carswell et al. 2016). The embedment reduction was also assumed to affect the effective stresses in the remaining soil adjacent to monopile due to loss of overburden.

2.3. Latin Hypercube sampling of stochastic model parameters

3

Model uncertainties have an important impact on all limit states for assessing structural performance of OWTs (Wilkie and Galasso 2020). To this end, stochastic assignment of model parameters was applied for all loads, OWT geometries, structural material properties, soil properties, and degradation properties. Latin Hypercube sampling (Olsson et al. 2003) was performed to generate 300 samples of near-random model parameters from a user-prescribed, correlation controlled multidimensional distribution (Fig. 3). The targeted probability distributions for model parameters were acquired from the literature (Wais 2017)(Ferreira and Guedes Soares 1999)(Hess et al. 2002)(Jones et al. 2002)(Matutano et al. 2013)(Han et al. 2019)(Momber 2016)(Garbatov et al. 2007). All randomly assigned model parameters were assumed to be uncorrelated, except for mean wind speeds and significant wave heights, between which a correlation coefficient of 0.85 (De Flippo 2015) was applied. Latin Hypercube sampling was repeated nine times for each run of fragility analysis aimed for different OWT ages.

2.4. Cloud-based multi-hazard fragility analyses

Nine cloud-based fragility analyses were performed for the OWT with age ranging from 0 to 40 years with a 5-year interval. Trained Gaussian Process Regression (GPR) model was used to process each set of logarithmic transformed cloud data, which consisted of one dependent variable, i.e., demand over capacity ratio, $\ln(Y)$, and two independent variables, i.e., wind and ground motion intensity measures (IM), $[\ln(S_a), \ln(V_{ave})]$, where S_a is ground motion spectral acceleration at the OWT's first natural period and V_{ave} is average wind speed (Zhang et al. 2022). The evaluated logarithmic mean and standard deviation across the desired range of prediction were then used to compute multivariable fragility functions.

3. Age-dependent multi-hazard fragility surfaces

Temporal evolution of ULS and SLS fragility surfaces of the OWT from 0 to 40 years are compared side by side in Fig. 4. At a given age, the fragility of the OWT is always higher when the ground motion IM $S_a(T_1)$ is larger and when the wind IM V_{ave} takes a value closer to the OWT's rated wind speed of 11.4 m/s. The rate of multi-hazard fragility deterioration initiated fast, especially in the first five years of the OWT's service life, and then gradually decreased over time. Within the range of examined wind – ground motion IMs, deterioration was more evidently reflected for spectral acceleration values near a design-level spectral acceleration of 0.189 g (calculated according to Eurocode 8 assuming reference peak ground acceleration on type A ground $a_{gR} = 0.5$ g), and for wind speeds laid in the mid- to upper-range of the OWT's operational limit. The relative variation of fragility was observed larger for ULS as compared to SLS. Relative change of failure probabilities with regard to age is also compared at two locations in Table 1, one representing design-level hazards and the other the extreme. Given design-level load combinations, the OWT's probability of exceeding SLS increased a third, and its probability of exceeding ULS doubled at the end of a typical 25-year design life.
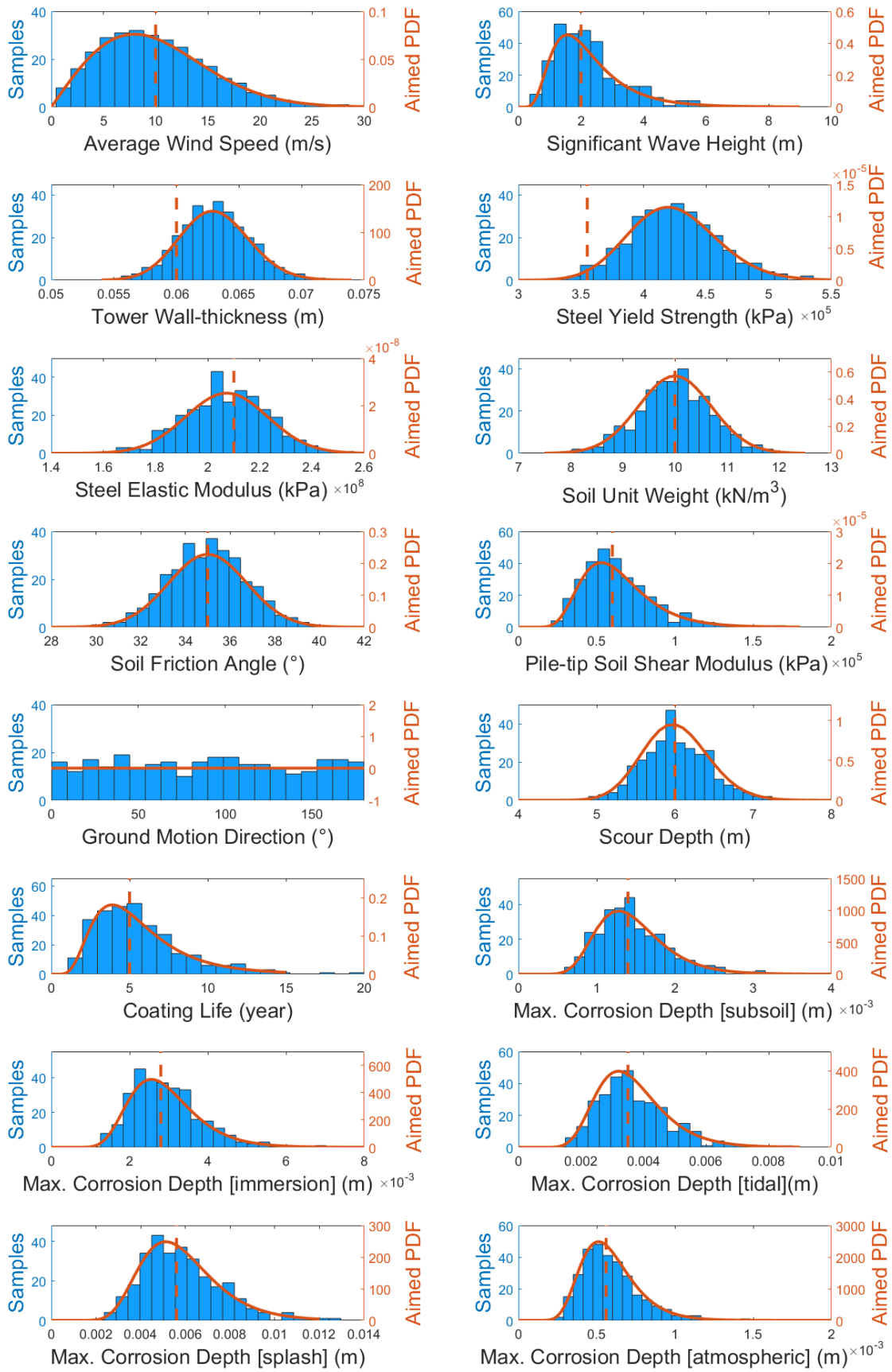
Fig. 3 – Latin hypercube sampling of the sixteen stochastically assigned model parameters. Note: the orange solid curves are the targeted probability density functions (PDF), the orange dashed lines mark nominal values taken for each model parameters (except for the uniformly distributed earthquake directionality), and the blue bins represent 300 generated samples.

Table 1. Temporal evolution of P(Y > 1|[0.189 g, 11.4 m/s]) and P(Y > 1|[0.4 g, 11.4 m/s]).

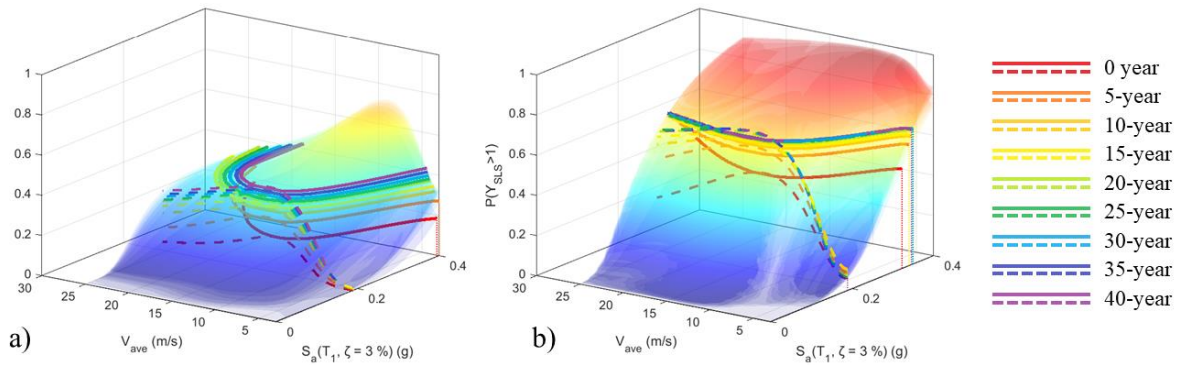| time (year)	ULS				SLS			
	$P(Y_{ULS} > 1|[0.189$ g, 11.4 m/s])		$P(Y_{ULS} > 1|[0.4$ g, 11.4 m/s])		$P(Y_{SLS} > 1|[0.189$ g, 11.4 m/s])		$P(Y_{SLS} > 1|[0.4$ g, 11.4 m/s])	
	value	variation to 0-year	value	variation to 0-year	value	variation to 0-year	value	variation to 0-year
0	0.1894	-	0.6401	-	0.4961	-	0.9423	-
5	0.2697	42%	0.6258	-2%	0.6015	21%	0.9588	2%
10	0.3150	66%	0.6396	0%	0.6391	29%	0.9645	2%
15	0.3393	79%	0.6538	2%	0.6511	31%	0.9688	3%
20	0.3644	92%	0.6613	3%	0.6645	34%	0.9716	3%
25	0.3735	97%	0.6618	3%	0.6700	35%	0.9731	3%
30	0.3890	105%	0.6694	5%	0.6730	36%	0.9743	3%
35	0.4059	114%	0.6729	5%	0.6742	36%	0.9738	3%
40	0.4241	124%	0.6796	6%	0.6745	36%	0.9734	3%

Fig. 4 – Temporal evolution of wind – ground motion fragility surfaces: a) ULS, b) SLS. Note: on each subfigure, the dashed curves are equal-$S_a(T_1, \zeta)$ marks referencing the Eurocode 8 design-level elastic spectral acceleration of the OWT $S_e(T \cong 4.0$ s, $\zeta = 3$ %) = 0.189 g, the solid curves are isopleths with $P(Y > 1) \equiv P(Y > 1|[0.189$ g, 11.4 m/s]).

4. Conclusions

This study presents age-dependent multi-hazard fragility functions of an operational monopile-supported NREL 5 MW OWT when subjected to combined loads of wind, wave and earthquake. A dual-IM cloud-based fragility assessment procedure was utilised to produce fragility surfaces from 0 to 40 years. Over time, the multi-hazard fragility of an ageing OWT degrades significantly with respect to its original state. The following key observations can be summarised:

- The rate of deterioration is age-dependent. A high rate of fragility increase is expected at the beginning stage of OWT's service time from 0 to 5 years.

- The OWT multi-hazard fragility deterioration is most noticeable for a design-level ground motion intensity combined with wind speeds around and above the OWT's rated value.

- Compared to its healthy counterpart, the probability of failure of a 25-year-old OWT's subjected to simultaneous code-based design-level wind, wave and seismic loads increases by a factor of 2.0.

References

Asareh M-A, Schonberg W, Volz J (2016) Fragility analysis of a 5-MW NREL wind turbine considering aero-elastic and seismic interaction using finite element method. Finite Elements in Analysis and Design 120:57–67. https://doi.org/10.1016/j.finel.2016.06.006

Bisoi S, Haldar S (2014) Dynamic analysis of offshore wind turbine in clay considering soil-monopile-tower interaction. Soil Dynamics and Earthquake Engineering 63:19–35. https://doi.org/10.1016/j.soildyn.2014.03.006

Carswell W, Arwade SR, DeGroot DJ, Myers AT (2016) Natural frequency degradation and permanent accumulated rotation for offshore wind turbine monopiles in clay. Renewable Energy 97:319–330. https://doi.org/10.1016/j.renene.2016.05.080

CEN (European Committee for Standardisation) (2007) Eurocode 3: Design of steel structures - Part 1-6: Strength and stability of shell structures. EN 1993-1-6: 2007 (E), Brussels

De Flippo M (2015) An Innovative Breakwater at Hanstholm harbour. Aalborg University

De Risi R, Bhattacharya S, Goda K (2018) Seismic performance assessment of monopile-supported offshore wind turbines using unscaled natural earthquake records. Soil Dynamics and Earthquake Engineering 109:154–172. https://doi.org/10.1016/j.soildyn.2018.03.015

DNV (2007) Design of Offshore Wind Turbine Structures. DNV-OS-J101, Norway

Do TQ, van de Lindt JW, Mahmoud H (2015) Fatigue Life Fragilities and Performance-Based Design of Wind Turbine Tower Base Connections. Journal of Structural Engineering 141:04014183. https://doi.org/10.1061/(ASCE)ST.1943-541X.0001150

Ferreira JA, Guedes Soares C (1999) Modelling the long-term distribution of significant wave height with the Beta and Gamma models. Ocean Engineering 26:713–725. https://doi.org/10.1016/S0029-8018(98)00022-5

Garbatov Y, Guedes Soares C, Wang G (2007) Nonlinear Time Dependent Corrosion Wastage of Deck Plates of Ballast and Cargo Tanks of Tankers. Journal of Offshore Mechanics and Arctic Engineering 129:48–55. https://doi.org/10.1115/1.2426987

Gelagoti FM, Kourkoulis RS, Georgiou IA, Karamanos SA (2019) Soil–Structure Interaction Effects in Offshore Wind Support Structures Under Seismic Loading. Journal of Offshore Mechanics and Arctic Engineering 141:1–15. https://doi.org/10.1115/1.4043505

Ghosh J, Padgett JE (2010) Aging Considerations in the Development of Time-Dependent Seismic Fragility Curves. Journal of Structural Engineering 136:1497–1511. https://doi.org/10.1061/(ASCE)ST.1943-541X.0000260

Han X, Yang DY, Frangopol DM (2019) Time-variant reliability analysis of steel plates in marine environments considering pit nucleation and propagation. Probabilistic Engineering Mechanics 57:32–42. https://doi.org/10.1016/j.probengmech.2019.05.003

Hess PE, Bruchman D, Assakkaf IA, Ayyub BM (2002) Uncertainties in Material and Geometric Strength and Load Variables. Naval Engineers Journal 114:139–165. https://doi.org/10.1111/j.1559-3584.2002.tb00128.x

Jones AL, Kramer SL, Arduino P (2002) Estimation of Uncertainty in Geotechnical Properties for Performance-Based Earthquake Engineering. Pacific Earthquake Engineering Research Center, University of California, Berkeley, CA, USA

Jonkman J, Butterfield S, Musial W, Scott G (2009) Definition of a 5-MW Wind Turbine Reference for Offshore System Development. Colorado, USA

Katsanos EI, Sanz AA, Georgakis CT, Thöns S (2017) Multi-hazard response analysis of a 5MW offshore wind turbine. Procedia Engineering 199:3206–3211. https://doi.org/10.1016/j.proeng.2017.09.548

Katsanos EI, Sextos AG, Elnashai AS (2014) Prediction of inelastic response periods of buildings based on intensity measures and analytical model parameters. Engineering Structures 71:161–177. https://doi.org/10.1016/j.engstruct.2014.04.007

Lai Y, Wang L, Hong Y, He B (2020) Centrifuge modeling of the cyclic lateral behavior of large-diameter monopiles in soft clay: Effects of episodic cycling and reconsolidation. Ocean Engineering 200:107048. https://doi.org/10.1016/j.oceaneng.2020.107048

Martín del poCam JO, Pozos-Estrada A (2020) Multi-hazard fragility analysis for a wind turbine support structure: An application to the Southwest of Mexico. Engineering Structures 209:1–11. https://doi.org/10.1016/j.engstruct.2019.109929

Matutano C, Negro V, López-Gutiérrez J-S, Esteban MD (2013) Scour prediction and scour protections in offshore wind farms. Renewable Energy 57:358–365. https://doi.org/10.1016/j.renene.2013.01.048

McKenna F (2011) OpenSees: A Framework for Earthquake Engineering Simulation. Computing in Science & Engineering 13:58–66. https://doi.org/10.1109/MCSE.2011.66

Melchers RE (1999) Corrosion uncertainty modelling for steel structures. Journal of Constructional Steel Research 52:3–19. https://doi.org/10.1016/S0143-974X(99)00010-3

Momber AW (2016) Quantitative performance assessment of corrosion protection systems for offshore wind power transmission platforms. Renewable Energy 94:314–327. https://doi.org/10.1016/j.renene.2016.03.059

NREL (2020) Main repository for the NREL-supported OpenFAST whole-turbine simulation code. https://github.com/OpenFAST/openfast. Accessed 30 Jul 2020

Olsson A, Sandberg G, Dahlblom O (2003) On Latin hypercube sampling for structural reliability analysis. Structural Safety 25:47–68. https://doi.org/10.1016/S0167-4730(02)00039-5

Papi F, Balduzzi F, Ferrara G, Bianchini A (2021) Uncertainty quantification on the effects of rain-induced erosion on annual energy production and performance of a Multi-MW wind turbine. Renewable Energy 165:701–715. https://doi.org/10.1016/j.renene.2020.11.071

Price S, Figueira R (2017) Corrosion Protection Systems and Fatigue Corrosion in Offshore Wind Structures: Current Status and Future Perspectives. Coatings 7:1–51. https://doi.org/10.3390/coatings7020025

Qin S, Cui W (2003) Effect of corrosion models on the time-dependent reliability of steel plated elements. Marine Structures 16:15–34. https://doi.org/10.1016/S0951-8339(02)00028-X

Ramachandran GK V, Vita L, Krieger A, Mueller K (2017) Design Basis for the Feasibility Evaluation of Four Different Floater Designs. Energy Procedia 137:186–195. https://doi.org/10.1016/j.egypro.2017.10.345

Rezamand M, Kordestani M, Carriveau R, et al (2020) Critical Wind Turbine Components Prognostics: A Comprehensive Review. IEEE Transactions on Instrumentation and Measurement 69:9306–9328. https://doi.org/10.1109/TIM.2020.3030165

Wais P (2017) Two and three-parameter Weibull distribution in available wind power analysis. Renewable Energy 103:15–29. https://doi.org/10.1016/j.renene.2016.10.041

Wilkie D, Galasso C (2020) Site-specific ultimate limit state fragility of offshore wind turbines on monopile substructures. Engineering Structures 204:109903. https://doi.org/10.1016/j.engstruct.2019.109903

WindEurope (2020) Offshore wind in Europe – key trends and statistics 2019. Brussels, Belgium

Yang Y, Wu Q, He Z, et al (2019) Seismic Collapse Performance of Jacket Offshore Platforms with Time-Variant Zonal Corrosion Model. Applied Ocean Research 84:268–278. https://doi.org/10.1016/j.apor.2018.11.015

Zhang Z, De Risi R, Sextos A (2022) Recommended regression models and intensity measure pairs for offshore wind turbine multi-hazard fragility functions (submitted). In: 3rd European Conference on Earthquake Engineering & Seismology. Bucharest, Romania, pp 1–10

Zheng XY, Li H, Rong W, Li W (2015) Joint earthquake and wave action on the monopile wind turbine foundation: An experimental study. Marine Structures 44:125–141. https://doi.org/10.1016/j.marstruc.2015.08.003